SSCL-615

SSCL-615
December 1992
Distribution Category: 414

V. Thiagarajan

The Longitudinal Coupling Impedance of a Slot on the SSC Collider Liner

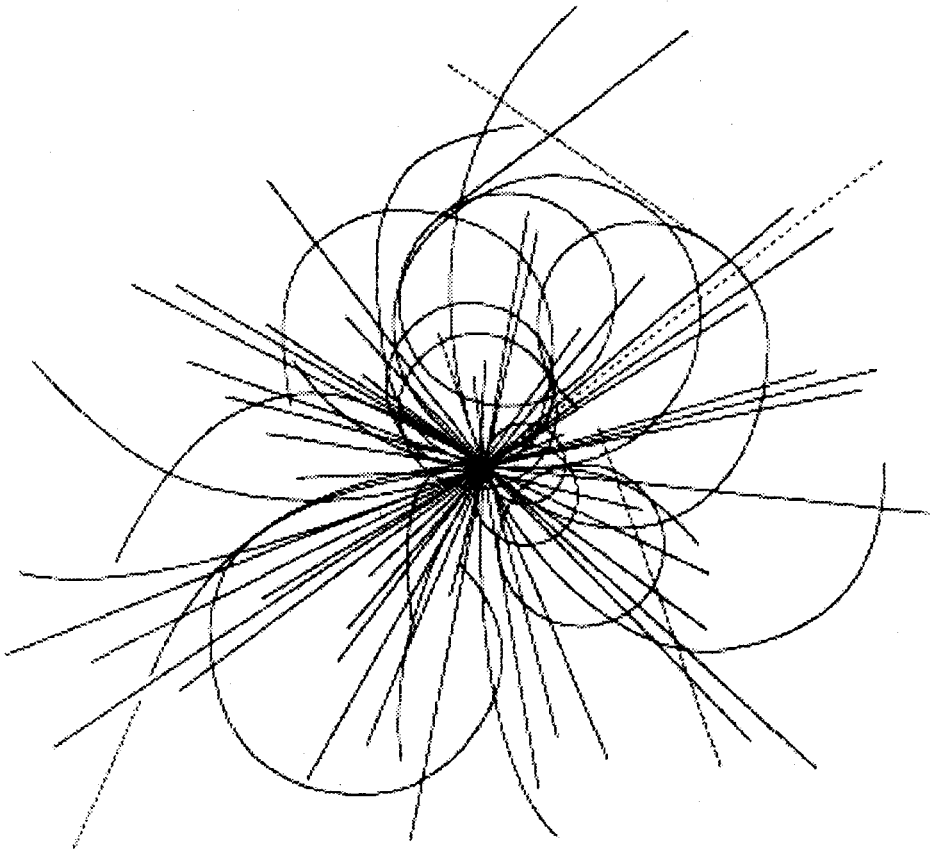

Superconducting Super Collider Laboratory

SSCL-615

The Longitudinal Coupling Impedance of a Slot on the SSC Collider Liner

V. Thiagarajan

Superconducting Super Collider Laboratory*
2550 Beckleymeade Avenue
Dallas, TX 75237

December 1992

* Operated by the Universities Research Association, Inc., for the U.S. Department of Energy under Contract No. DE-AC35-89ER40486.

The Longitudinal Coupling Impedance of a Slot on the SSC Collider Liner

V. Thiagarajan

Abstract

The location of a liner inside the Collider beam tube is under study at the Superconducting Super Collider Laboratory. The purpose of the liner is two-fold. It will be at a temperature higher than that of the beam tube and will help remove the synchrotron radiation energy from the 20-TeV proton beam, thus reducing the load on the cryogenic system. The liner is also designed to enhance the vacuum toward higher beam currents and luminosities. A definite distribution of holes (or slots) with the required pumping area needs to be located on the surface of the liner to maintain the vacuum. On the negative side, there will be diffracted wake fields following the beam fields incident on the pumping holes. These wake fields may attenuate with distance or propagate, depending on the frequency. They will cause longitudinal and transverse forces on the following bunches of protons and may result in coherent multi-bunch instabilities, as well as cause bunch lengthening and emittance growth. The effect of the wake fields may be expressed through the longitudinal and transverse coupling impedances, which are defined proportional to the corresponding forces integrated through distance, per unit charge. This report describes a method to evaluate the longitudinal coupling impedance of slots or holes of given dimensions on the liner, as a function of the frequency in the range 0 to approximately 100 GHz, in order to facilitate optimum choice of slots or holes on the liner.

CONTENTS

FIGURES vii
TABLES vii
1.0 INTRODUCTION 1
2.0 DESCRIPTION OF THE PROBLEM 2
3.0 WAVEGUIDE NORMAL MODE ANALYSIS 3
4.0 BOUNDARY CONDITIONS 5
5.0 RADIATED FIELDS IN THE LINER 8
6.0 NORMALIZATION OF FIELDS 8
7.0 THE LONGITUDINAL COUPLING IMPEDANCE 10
7.1 Longitudinal Impedance in the Low-Frequency Limit 12
7.2 Impedance at High Frequencies 12
8.0 RESULTS AND DISCUSSION 13
ACKNOWLEDGEMENTS 17
REFERENCES 19

FIGURES

1. Slot Details and Coordinate System. 2
2. Bessel Functions J_0 and J_1. 6
3. Slot Coordinates and Transformations. 10
4. Impedance vs. Frequency for Slots of Various Sizes. 13
5. Impedance vs. Frequency for Holes of Various Sizes. 14
6. Impedance vs. Frequency—Slots and Holes Compared. 14
7. Longitudinal Impedance for 2-mm Hole. (a) Real part; (b) Imaginary part. . . . 15
8. Longitudinal Impedance for 4 mm×2 mm Slot. (a) Real part; (b) Imaginary part. 15

TABLES

1. Normal Modes for a Round Tube. 5

1.0 INTRODUCTION

The Superconducting Super Collider (SSC) beam will have an energy of 20 TeV. At this high energy, there will be synchrotron radiation to reckon with, even though this is a proton beam. The collider is being designed for high beam currents and luminosities, with future upgrades in mind. Therefore, the location of a liner inside the beam tube is under study at the SSC Laboratory. The liner will be maintained at a temperature higher than that of the beam pipe; it will serve as a synchrotron-radiation intercept with high efficiency and will also help enhance the vacuum. We need to provide pumping holes, or slots, on the liner for the removal of desorbing gases. As a bunch of protons traverses inside the liner, the electromagnetic fields due to this source will be incident on the pumping holes. There will be diffracted wake fields that may attenuate or propagate with distance, depending on the frequency. These wake fields will act on successive bunches, causing bunch lengthening, emittance growth, or coherent instabilities, depending on the wake fields and their frequency dependence, or depending indirectly on the geometry and distribution of slots or holes on the liner.

The effect of the wake fields may be expressed quantitatively through the longitudinal or transverse coupling impedance of holes or slots, which are defined proportional to the integrated force (longitudinal or transverse) per unit charge.[1–4] There have been analyses of coupling impedances due to discontinuities and enlargements on the beam pipe (bellows, rf cavities, *etc.*). The coupling impedance of holes/slots on the liner for the Large Hadron Collider (LHC) at CERN and the SSC liner have been studied by Gluckstern[5] and Kurennoy,[6] who have obtained similar expressions for the coupling impedances valid at low frequencies. Gluckstern uses an approach based on Fourier-decomposed fields, while Kurennoy uses a normal mode series method; both describe the wake fields in terms of the polarizability and magnetization of the slots or holes obtained from electrostatic analyses. An exact expression for the magnetic vector potential due to a current source oscillating sinusoidally in infinite space can be found in Jackson.[7] He has shown that at low frequencies, the radiation pattern can be described to the lowest two orders, by a polarizability $\vec{P}$, magnetization $\vec{M}$, and a quadrupole moment tensor $\vec{\vec{Q}}$. But it is not known how the solution will be affected by a boundary such as the liner wall surrounding the oscillating source.

The wake fields and coupling impedances can, of course, be studied numerically using codes such as MAFIA,[8] but this approach suffers from the limitation that we cannot find the effect of parameters on the results without enormous and lengthy computations. The purpose of this paper is to derive a semi-analytic expression for the longitudinal coupling impedance of slots on the SSC collider liner, valid for a large range of frequencies (such

as 0–100.0 GHz). The method we present is equally applicable to holes. We will employ a series approach using waveguide normal modes described in Collin.[9] We will keep the analysis electrodynamic and solve the problem with approximate boundary conditions.

2.0 DESCRIPTION OF THE PROBLEM

A schematic of the beam pipe and the liner is shown in Figure 1. The liner of inner radius a and thickness Δ is located inside the beam pipe of inner radius b. A slot of length w and width d is located on the liner. The center of the slot is at $z = 0$. Our analysis is valid for round holes also, and we will use d to denote the diameter of the hole. The coordinate system is also shown in Figure 1. A single charge q travels along the axis of the liner with the speed of light c, and the field at the slot is given by

$$E_r^b = \frac{q}{2\pi\epsilon_0 a}\delta(z - ct)\,. \tag{1}$$

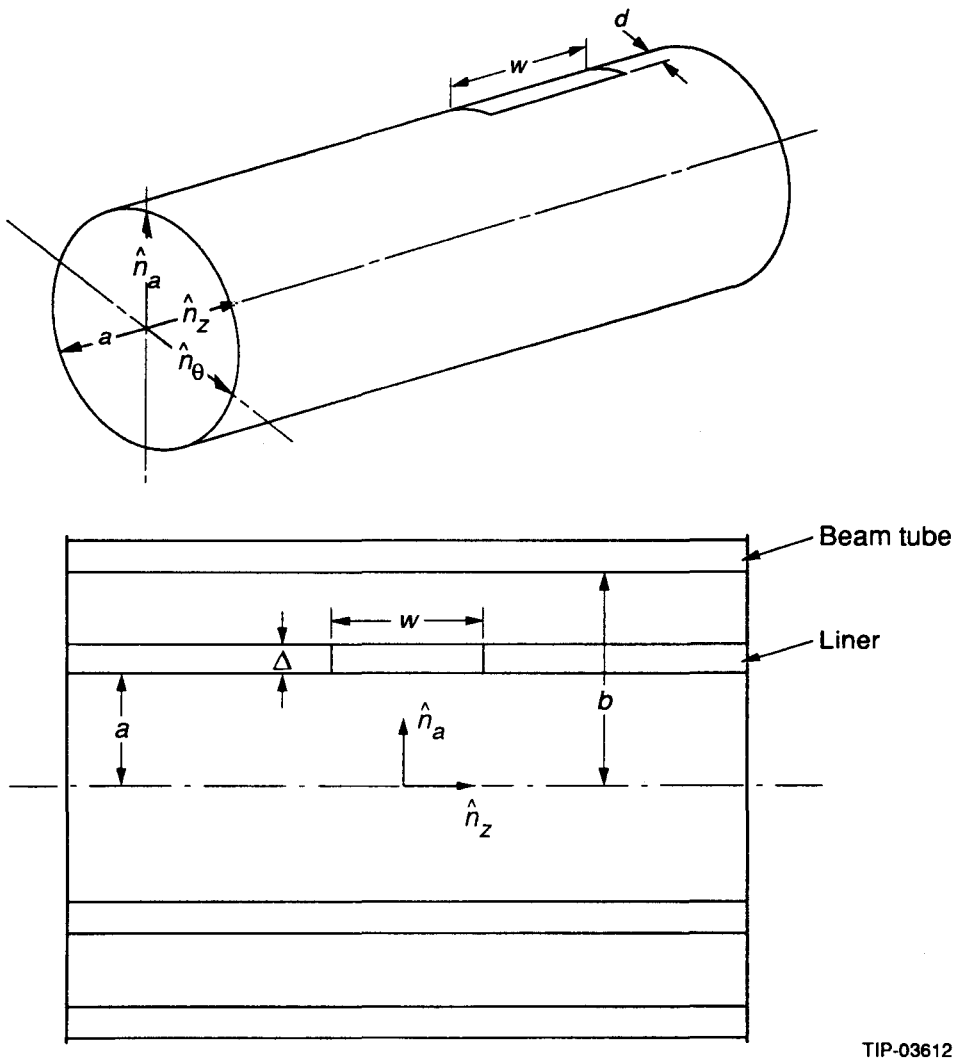

Figure 1. Slot Details and Coordinate System.

If we Fourier transform Eq. (1) with $f(\omega) = \int f(t)\exp(j\omega t)dt$, we obtain

$$E_r^b(\omega) = \frac{Z_0 q}{2\pi a} \exp(-jkz) . \tag{2}$$

In Eq. (2), $Z_0 = 120\pi$ is the impedance of free space. Our task is to calculate the diffracted field and its propagation inside the liner due to the incident field given by Eq. (2). We will use the following method outlined in Collin,[9] which is a modification of the theory illustrated by Bethe.[10] In step 1, we will introduce a magnetic wall at the slot at $r = a$. This implies that the magnetic intensity H_z and the normal field E_n at the slot are equal to zero. We can solve for the radiated field inside the liner (Region I). The Maxwell's equation $\nabla \times E = \frac{-\partial B}{\partial t}$ will not be satisfied at the slot. There will be an imbalance, which we will call the magnetic current density J_m. In step 2, we will remove the magnetic wall and introduce a magnetic current density $-J_m$ at the slot. There will be radiation in Region I and also in the annular region bounded by the beam pipe, which we will call Region II. The solution for Region I will be the sum of the beam field and the solutions obtained in steps 1 and 2. The solution for Region II will be the solution obtained in step 2. We can make a further simplification in step 2. If we assume symmetric radiation from the current element at the slot, we can say that the radiation in Regions I and II is due to two current elements at the slot, each being equal to $-J_m/2$. We can further simplify the problem for the radiation in Region I alone by calculating a radiation field due to a current density $J_m - J_m/2 = J_m/2$. Collin[9] has shown that this corresponds to Bethe's[10] approach. We will adopt this method, and our problem reduces to introducing a magnetic wall at the slot, calculating the wakefields and impedances, and dividing the result by 2.

3.0 WAVEGUIDE NORMAL MODE ANALYSIS

The charge relaxation time is given by $\frac{\sigma}{\epsilon_0}$. The skin depth for oscillating currents is given by $\sqrt{\frac{2}{\mu\sigma\omega}}$. The conductivity σ for metals is of the order of 10^8 S/m; assuming a frequency of 1 GHz, the charge relaxation time is found to be about 10^{-18} sec and the skin depth is found to be of the order of a few microns. We will be dealing in time scales much greater than the charge relaxation time and dimensions much greater than the skin depth. Under these conditions we can use waveguide solutions for our problem. We will treat the beam pipe and the slot as waveguides and apply continuity criteria at the interface.

There are two possible modes of propagation inside the beam pipe—the transverse magnetic mode (TM) and the transverse electric (TE). The TM mode alone produces an axial electric field at $r = 0$, and hence contributes to longitudinal impedance. Therefore, we will deal only with the TM mode. The waveguide normal modes are derived in texts on

electromagnetic theory. We will follow the notation convention in Plonsey and Collin.[11] We will assume a time variation of $e^{j\omega t}$ and a z variation of $e^{-j\beta z}$, where ω and β are the rotational frequency and the propagation factor, respectively. The coordinate system is shown in Figure 1. The component e_z satisfies the Helmholtz equation:

$$\nabla_t{}^2 e_z \; + k_c{}^2 e_z \; = \; 0\,, \tag{3}$$

where

$$\beta^2 \; = \; k^2 - k_c{}^2\,, \; k = \frac{\omega}{c}\,. \tag{4}$$

The solution of Eq. (3) obtained by separation of variables is

$$e_z \; = \; J_n(k_c r)\,\Big(A\;\cos(n\theta) \; + \; B\;\sin(n\theta)\Big)\,. \tag{5}$$

The J_n is the Bessel function of order n with parameter k_c. We can anticipate (from the definition of longitudinal impedance) that $n = 0$ alone contributes to the longitudinal impedance, while all the modes $n = 0, 1, 2\ldots$ will affect the boundary conditions. The field at the metallic wall at $r = a$ is zero to satisfy the boundary condition. This implies

$$J_n(k_c a) \; = \; 0\,. \tag{6}$$

There is an infinite number of solutions p_{nm} for Eq. (6), with

$$p_{nm} = k_c a\,, \qquad m = 1, 2, 3\ldots\,. \tag{7}$$

The corresponding propagation factor is given by

$$\beta_{nm} = \pm\sqrt{k^2 - \frac{p_{nm}{}^2}{a^2}}\,. \tag{8}$$

We have to choose an appropriate sign for β_{nm} depending on the physical situation. The TM normal modes for a round tube are listed in Table 1. Those for a rectangular geometry can be found in Reference 11. We will need the propagation factor for the rectangular geometry when we study rectangular slots. For a rectangle with sides $2a_1, 2b_1$,

$$\beta_{nm} \; = \; \pm\sqrt{k^2 - (\frac{n\pi}{a_1})^2 - (\frac{m\pi}{b_1})^2}\,. \tag{9}$$

Table 1. Normal Modes for a Round Tube.

Component	Normal Mode
h_{nz}	0
e_{nz}	$J_n(p_{nm}\frac{r}{a})e^{\pm j\beta_{nm}z}\cos(n\theta)$
h_{nr}	$-\frac{e_{n\theta}}{Z_{e,nm}}$
$h_{n\theta}$	$\frac{e_{nr}}{Z_{e,nm}}$
e_{nr}	$\frac{-j\beta_{nm}p_{nm}}{ak^2_{c,nm}}J'_n(p_{nm}\frac{r}{a})e^{\pm j\beta_{nm}z}\cos(n\theta)$
$e_{n\theta}$	$\frac{-jn\beta_{nm}}{rk^2_{c,nm}}J_n(p_{nm}\frac{r}{a})e^{\pm j\beta_{nm}z}(-\sin(n\theta))$
β_{nm}	$\pm(k^2-\frac{p^2_{nm}}{a^2})^{\frac{1}{2}}$
$Z_{e,nm}$	$\frac{\beta_{nm}}{k}Z_0$
Z_0	$(\frac{\mu_0}{\epsilon_0})^{\frac{1}{2}}$
$k_{c,nm}$	$\frac{p_{nm}}{a}$

4.0 BOUNDARY CONDITIONS

We have already used one boundary condition (Eq. (6)). We shall begin with the discussion of the boundary condition at the slot. We will discuss the component E_z at the slot. Once this is determined every other component will follow through the relations among normal modes that stem from Maxwell's equations. Though E_z is equal to zero at the wall of the liner at $r = a$, it is non-zero at the slot. Waves propagate along r (along the axis of the slot) into the coaxial region bounded by the beam pipe. The fields have to satisfy the Helmholtz equation, and therefore the solutions will be those given in Table 1 for a round tube (or those given in Reference 11 for a rectangular slot). The axial and radial components of the fields are governed by the Bessel functions, $J_n(x), J'_n(x)$. The behavior of these functions is shown in Figure 2 for $n = 0$. From the properties of Bessel functions $J_0{}'(x) = -J_1(x)$. Therefore, when $J_0{}'(x) = 0$, $J_1(x)$ goes through an extremum. The roots of $J_n(x) = 0$ give the fields everywhere at $r = a$ except at the slot. In order to describe the field at the slot, we need to determine an argument of the Bessel functions different from p_{nm}. The fields on the liner side of the slot will be governed by a propagation factor determined with the radius of the liner, while the fields at the slot on the interior side of the slot will be determined by a propagation factor β^s, which will depend on the slot dimensions. These fields will have to have the same value and slope at the slot. This condition yields the following equation, which will help us determine a Bessel argument to determine the fields at the slot:

$$\frac{1}{E_z}\frac{\partial E_z}{\partial r}\bigg|_{\text{liner}} = \frac{1}{E_z}\frac{\partial E_z}{\partial r}\bigg|_{\text{slot}}. \tag{10}$$

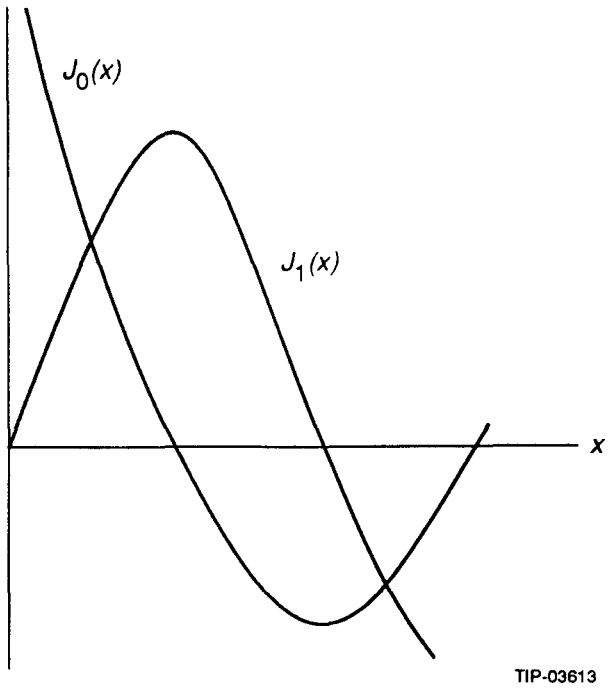

Figure 2. Bessel Functions J_0 and J_1.

Since other field components are determined from E_z, Eq. (10) will ensure the continuity of other field components as well. E_z will be a weighted sum of normal modes given by

$$E_z = \sum\sum A_{nm} e_{z,nm} \,. \tag{11}$$

The weights A_{nm} are yet to be determined. The propagation factor β^s for the slot will be large, and we will consider just the fundamental. The waves will be damped inside the slot.

$$\frac{1}{E_z}\frac{\partial E_z}{\partial r}\bigg|_{\text{slot}} = \frac{1}{e_z}\frac{\partial e_z}{\partial r}\bigg|_{\text{slot}} = -\beta^s \,. \tag{12}$$

Let us consider the following equation:

$$\frac{1}{e_{z,nm}}\frac{\partial e_{z,nm}}{\partial r}\bigg|_{\text{liner}} = \frac{1}{e_z}\frac{\partial e_z}{\partial r}\bigg|_{\text{slot}} = -\beta^s \,. \tag{13}$$

Consider also,

$$\frac{1}{e_{z,nm}}\frac{\partial e_{z,nm}}{\partial r}\bigg|_{\text{liner}} = \frac{J_n{}'(P_{nm}r/a)}{J_n(P_{nm}r/a)}\bigg|_{r=a} = -\beta^s \,. \tag{14}$$

The argument of the Bessel functions contains P_{nm} to distinguish it from p_{nm}, which makes the fields zero at the wall. The following equation for P_{nm} results from Eq. (14):

$$P_{nm} J_n'(P_{nm}) + a\beta^s \, J_n(P_{nm}) = 0 \,. \tag{15}$$

We can solve Eq. (15) for an infinite set of P_{nm} for $n = 0, 1, 2, 3\ldots$ and $m = 1, 2, 3\ldots$, depending on the radius a of the liner and β^s, which depends on the dimensions of the slot through Eqs. (8) and (9). When the slot dimensions are infinitely small, β^s becomes infinitely large, and Eq. (15) reduces to Eq. (6). Also, Eq. (15) yields a relation between J_0 and J_1 for $n = 0$ and $n = 1$. We will stop with $n = 1$ and $m = 39$ in the numerical computations.

We need to satisfy Eq. (10) to maintain continuity of the fields at the slot. From Eqs. (10) and (11),

$$\frac{1}{E_z}\frac{\partial E_z}{\partial r}\bigg|_{\text{liner}} = \frac{\sum\sum A_{nm}\frac{\partial e_{z,nm}}{\partial r}}{\sum\sum A_{nm}e_{z,nm}}. \tag{16}$$

If we choose $A_{nm} = A$ and use the property of proportional fractions, we find that Eq. (10) is satisfied. We can assume without loss of generality that $A = 1$. We can introduce a constant later.

The introduction of the magnetic wall at the slot results in the following boundary conditions. We will use a subscript s to denote the diffracted (radiated) fields.

$$E_{sr} = \hat{n}_a.E_s = -E_r^b = \frac{-Z_0 q}{2\pi a}e^{-jkz}. \tag{17}$$

Using the ratio of the normal modes with P_{nm} as the Bessel argument, we get

$$E_{sz} = \frac{Z_0 q}{2\pi a}e^{-jkz}\frac{[J_0(P_{01}) + J_0(P_{02}) + \ldots]}{j[\frac{\beta_{01}a}{P_{01}}J_1(P_{01}) + \frac{\beta_{02}a}{P_{02}}J_1(P_{02}) + \ldots \frac{\beta_{11}a}{P_{11}}J_1(P_{11}) + \frac{\beta_{12}a}{P_{12}}J_1(P_{12}) + \ldots]}. \tag{18}$$

It should be noted that the denominator of Eq. (18) will be summed over $n = 0, 1$, while the numerator will be summed over just $n = 0$, because $n = 1, 2, \ldots$, do not contribute to the longitudinal impedance. We can also identify A, described earlier, with the right-hand side of Eq. (18) divided by $[J_0(P_{01}) + J_0(P_{02}) + \ldots]$. Also the β's in Eq. (18) are to be evaluated with P_{nm}'s.

For low frequencies, $j\beta_{nm} = |\beta_{nm}| \approx \frac{P_{nm}}{a}$. Therefore, Eq. (18) can be simplified as

$$E_{sz} = \frac{Z_0 q}{2\pi a}e^{-jkz}\frac{[J_0(P_{01}) + J_0(P_{02}) + \ldots]}{[J_1(P_{01}) + J_1(P_{02}) + \cdots + J_1(P_{11}) + J_1(P_{12}) + \ldots]}. \tag{19}$$

For high frequencies, β_{1m} will be real and its sign will be determined to keep the real part of impedance positive for every m. E_{sz} is given by

$$E_{sz} = \frac{Z_0 q}{2\pi a}e^{-jkz}\frac{[J_0(P_{01}) + J_0(P_{02}) + \ldots]}{j[J_1(P_{01}) + J_1(P_{02}) + \cdots + J_1(P_{11}) + J_1(P_{12}) + \ldots]}. \tag{20}$$

It should be remembered that Eqs. (18)–(20) describe the diffracted fields at the slot at $r = a$. The magnetic current at the slot is given by the following equation:[9]

$$\nabla \times E \;=\; -J_m \,. \tag{21}$$

This implies

$$J_m \;=\; -\hat{n}_a \times E_s \;=\; \hat{n}_\theta E_{sz} - \hat{n}_z E_{s\theta} \,. \tag{22}$$

5.0 RADIATED FIELDS IN THE LINER

In Section 4.0, we derived expressions for the diffracted field and the magnetic current at the slot. We can consider the J_m as an oscillating source of radiation and compute the radiated fields in the liner using the Lorentz reciprocity theorem.[9] The radiated fields may be expanded using the waveguide normal modes (Table 1) as follows:

For $z > 0.0$,

$$E_s = \sum a_n E_n^+ \;=\; \sum a_n(\hat{n}_a e_{nr} + \hat{n}_\theta e_{n\theta} + \hat{n}_z e_{nz})\; e^{-j\beta_{nm}z} \cos(n\theta)\,, \tag{23}$$

$$H_s = \sum a_n H_n^+ \;=\; \sum a_n(\hat{n}_a h_{nr} + \hat{n}_\theta h_{n\theta} + \hat{n}_z h_{nz})\; e^{-j\beta_{nm}z} \cos(n\theta)\,. \tag{24}$$

For $z < 0.0$,

$$E_s = \sum b_n E_n^- \;=\; \sum b_n(\hat{n}_a e_{nr} + \hat{n}_\theta e_{n\theta} - \hat{n}_z e_{nz})\; e^{+j\beta_{nm}z} \cos(n\theta)\,, \tag{25}$$

$$H_s = \sum b_n H_n^- \;=\; \sum b_n(-\hat{n}_a h_{nr} - \hat{n}_\theta h_{n\theta} + \hat{n}_z h_{nz})\; e^{+j\beta_{nm}z} \cos(n\theta)\,. \tag{26}$$

Equations (23)–(26) use appropriate sign conventions to make power flow positive in either positive or negative z directions.

6.0 NORMALIZATION OF FIELDS

We can normalize the electric, magnetic fields and distances by dividing by factors f V/m, f/z_e A/m, and a m, and carrying out the normalization such that $\int e_{nr} h_{n\theta} ds \;=\; 1.0$, where the area integral is carried out over the section of the liner. This gives

$$f_{0m}^2 = -\pi \frac{\beta_{om}^2}{k_{c,om}^2} J_1^2\left(p_{0m}\frac{r}{a}\right)\,. \tag{27}$$

The sign for f_{0m}^2 should be chosen such that power flow is positive in either direction. Using the Lorentz reciprocity theorem,[9]

$$\int\!\!\int (E_n^\pm \times H_s - E_s \times H_n^\pm)\hat{n} ds \;=\; \int\!\!\int\!\!\int (J.E_n^\pm - H_n^\pm.J_m) dv\,, \tag{28}$$

where the subscripts s and n denote the radiated fields and normal modes, respectively. J is the external current source, which is zero in our case; J_m is the magnetic current density, which is given by Eq. (22). Using Eqs. (23)–(27), we can obtain the following expressions for the coefficients a_n and b_n:

$$a_{nm} = \frac{1}{2}\int\int H_n^- . \hat{n}_\theta \; E_{sz} \frac{Z_e}{f_{0m}^2 a} \; d\theta \; dz \Big|_{\text{slot}} , \tag{29}$$

$$b_{nm} = \frac{1}{2}\int\int H_n^+ . \hat{n}_\theta \; E_{sz} \frac{Z_e}{f_{0m}^2 a} \; d\theta \; dz \Big|_{\text{slot}} . \tag{30}$$

We know the diffracted field E_{sz} at the slot from Eq. (19) or Eq. (20), and we can compute the coefficients a_{nm}, b_{nm}. We have generalized these coefficients with the addition of a subscript m to correspond to the Bessel modes. Equations (29) and (30) give us the coefficients for the field radiated by a current element located at $z = 0$. Our source spreads across the length of the slot from $z = -w/2$ to $z = +w/2$. We can consider this as a distribution of elemental sources, and the resulting coefficients for the radiated fields will require an integration over z. A sketch of the slot of length w located with center at $z = 0$ is shown in Figure 3(a). For convenience, we have also shown a transformed coordinate z', where $z' = z + w/2$. There will be radiation in the positive direction for $z' > 0$. At a particular location, say $z' = \zeta$, radiation will add up due to all elementary current elements to the left of ζ, *i.e.*, from $z' = 0$ to $z' = \zeta$. The field $H_{n\theta}^-$ at ζ due to a current element at z' is given by

$$H_{n\theta}^- = \frac{jk}{k_{c,nm}} \frac{1}{Z_0} \; J_n'(p_{nm}) \; \cos(n\theta) \; e^{j\beta_{nm}(\zeta - z')} , \tag{31}$$

$$E_{sz} = B \; e^{-jkz} = B \; e^{-j(kz' - w/2)} , \tag{32}$$

where B can be extracted from Eq. (19) or Eq. (20). The result after integration is

$$a_{nm}\Big|_{z<w/2} = \frac{1}{2\pi a^2} \phi B \frac{p_{nm}}{\beta_{nm}} \frac{J_n'(p_{nm})}{J_{n+1}^2(p_{nm})} e^{jkw/2} e^{j\beta_{nm}\zeta} \frac{1}{\beta_{nm} + k} \left[1.0 - e^{-j\zeta(\beta_{nm}+k)}\right] , \tag{33}$$

with $n = 0$ in our equations, and $\phi = d/w$. Equation (33) is valid in the range $z' = 0$ to w (or, $z = -w/2$ to $w/2$). At $z = w/2$, Eq. (33) reduces to

$$a_{nm}\Big|_{z=w/2} = \frac{1}{2\pi a^2} \phi B \frac{p_{nm}}{\beta_{nm}} \frac{J_n'(p_{nm})}{J_{n+1}^2(p_{nm})} e^{jkw/2} e^{j\beta_{nm}w} \frac{1}{\beta_{nm} + k} \left[1.0 - e^{-jw(\beta_{nm}+k)}\right] , \tag{34}$$

and for $z > w/2$,

$$a_{nm}\Big|_{z>w/2} = a_{nm}|_{z=w/2} e^{-j\beta_{nm}(z'-w)} . \tag{35}$$

In a similar fashion, the coefficients b_{nm} for radiation in the negative direction can be obtained. The sketch is shown in Figure 3(b). We can carry out the integrations to obtain the following expressions:

$$b_{nm}\Big|_{z>-w/2} = \frac{1}{2\pi a^2}\phi B \frac{p_{nm}}{\beta_{nm}} \frac{J_n'(p_{nm})}{J_{n+1}^2(p_{nm})} e^{-jkw/2} e^{-j\beta_{nm}\zeta} \frac{1}{\beta_{nm}-k} \left[1.0 - e^{-j\zeta(\beta_{nm}-k)}\right] , \tag{36}$$

$$b_{nm}\Big|_{z=-w/2} = \frac{1}{2\pi a^2}\phi B \frac{p_{nm}}{\beta_{nm}} \frac{J_n'(p_{nm})}{J_{n+1}^2(p_{nm})} e^{-jkw/2} e^{j\beta_{nm}w} \frac{1}{\beta_{nm}-k} \left[1.0 - e^{-jw(\beta_{nm}-k)}\right] , \tag{37}$$

$$b_{nm}\Big|_{z<-w/2} = b_{nm}|_{z=-w/2} e^{-j\beta_{nm}(z'+w)} . \tag{38}$$

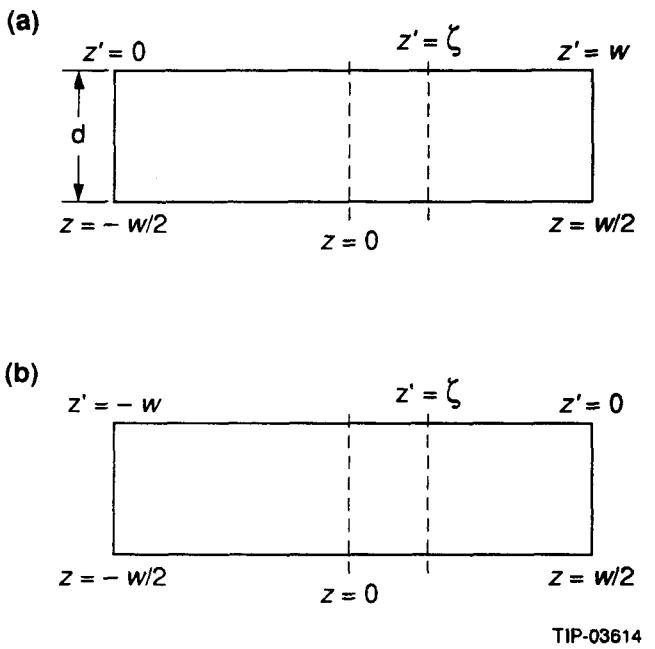

Figure 3. Slot Coordinates and Transformations.

7.0 THE LONGITUDINAL COUPLING IMPEDANCE

The longitudinal coupling impedance $Z(\omega)$ is defined as follows:[1–6]

$$Z(\omega) = -\frac{1}{q}\int_{-\infty}^{\infty} E_z(r=0,\theta=0)e^{-jkz}\, dz . \tag{39}$$

Since $J_0(0) = 1.0$, and since the z dependence has been absorbed in the integrations to obtain the coefficients a_{nm} and b_{nm}, $E_z = a_{nm}$ or b_{nm}. At high frequencies, the coefficients will be further multiplied by j; hence, $E_z(r=0,\theta=0)$ also will be multiplied by j and will

be given by ja_{nm} or jb_{nm}. We can carry out the integration in Eq. (39) in four parts. We will carry out the first and second integrals, $\mathcal{I}_1$ and $\mathcal{I}_2$, with a transformation $z' = z - w/2$ and with limits on z', $-\infty$ to $-w$ and $-w$ to 0; this will cover the radiation in the negative z direction.

The third and fourth part of the integrals $\mathcal{I}_3$ and $\mathcal{I}_4$, with a transformation $z' = z + w/2$ and with limits 0 to w and w to ∞ on z', can be carried out to cover the radiation in the positive direction. The result is

$$\mathcal{I}_1 = -\frac{1}{q}\frac{1}{2\pi a^2}\phi B\frac{p_{nm}}{\beta_{nm}}\frac{J_n'(p_{nm})}{J_{n+1}^2(p_{nm})}\frac{e^{j\beta_{nm}w}}{j(\beta_{nm}-k)^2}\left[1.0 - e^{-jw(\beta_{nm}-k)}\right], \tag{40}$$

$$\mathcal{I}_2 = -\frac{1}{q}\frac{1}{2\pi a^2}\phi B\frac{p_{nm}}{\beta_{nm}}\frac{J_n'(p_{nm})}{J_{n+1}^2(p_{nm})}\frac{e^{-jkw}}{(\beta_{nm}-k)}\left[\frac{1.0 - e^{-jw(\beta_{nm}+k)}}{-j(\beta_{nm}+k)} - \frac{1.0 - e^{2jkw}}{-2jk}\right]. \tag{41}$$

Expanding the exponentials within the square brackets and retaining terms up to order w, we find

$$\mathcal{I}_2 \approx 0. \tag{42}$$

In a similar fashion, we find

$$\mathcal{I}_3 \approx 0, \tag{43}$$

$$\mathcal{I}_4 = \frac{1}{q}\frac{1}{2\pi a^2}\phi B\frac{p_{nm}}{\beta_{nm}}\frac{J_n'(p_{nm})}{J_{n+1}^2(p_{nm})}\frac{e^{j\beta_{nm}w}}{j(\beta_{nm}+k)^2}\left[1.0 - e^{-jw(\beta_{nm}+k)}\right]. \tag{44}$$

Adding up the four-part integrals and summing over the Bessel mode m, we get the following expression for the longitudinal coupling impedance:

$$Z(\omega) = \sum_m -\frac{1}{q}\frac{1}{2\pi a^2}\phi B\frac{p_{nm}}{\beta_{nm}}\frac{J_n'(p_{nm})}{J_{n+1}^2(p_{nm})}e^{j\beta_{nm}w}\frac{2kwa^2}{{p_{nm}}^2}.$$

Further we need to divide the above expression for the impedance by 2 to account for half the J_m at the slot. Also, $\phi = d/a$; $J_0'(p_{nm}) = -J_1(p_{nm})$; and from Eqs. (19) and (20),

$$B = \frac{Z_0 q}{2\pi a}\frac{[J_0(P_{01}) + J_0(P_{02}) + \ldots]}{[J_1(P_{01}) + J_1(P_{02}) + \cdots + J_1(P_{11}) + J_1(P_{12}) + \ldots]}. \tag{45}$$

We get the following expression for the frequency-dependent longitudinal coupling impedance:

$$Z(\omega) = \sum_m \frac{Z_0 wdk}{4\pi^2 a^2}\frac{[J_0(P_{01}) + J_0(P_{02}) + \ldots]}{[J_1(P_{01}) + J_1(P_{02}) + \cdots + J_1(P_{11}) + J_1(P_{12}) + \ldots]}\frac{e^{j\beta_{nm}w}}{p_{0m}\beta_{nm}J_1(p_{0m})}. \tag{46}$$

It should be noted that P_{0m}'s are obtained from Eq. (15), and p_{om}'s from Eq. (6). The frequency dependence of the impedance occurs through k and β_{0m} through Eq. (4).

7.1 Longitudinal Impedance in the Low-Frequency Limit

In the low-frequency limit, $k \ll \frac{p_{0m}}{a}$, and from Eq. (8),

$$\beta_{0m} \approx \pm j\beta_{0m} . \tag{47}$$

It is understood that we will use the modulus of β_{0m} on the right-hand side of Eq. (47). The sign should be chosen so that the waves damp with z; *i.e.*, $\exp(-j\beta w) = \exp(-\beta w)$. Expanding the exponential, the expression for the impedance can be written as

$$Z(\omega) = \sum_m \frac{Z_0 w d k}{4\pi^2 a^2} \frac{[J_0(P_{01}) + J_0(P_{02}) + \ldots]}{[J_1(P_{01}) + J_1(P_{02}) + \cdots + J_1(P_{11}) + J_1(P_{12}) + \ldots]} \times \frac{1}{j}\left[\frac{1}{p_{0m}\beta_{0m}J_1(p_{0m})} - \frac{w}{p_{0m}J_1(p_{0m})} + \ldots\right] .$$

Or,

$$Z(\omega) = \left[\sum \frac{Z_0 w d k}{4\pi^2 a^2}\frac{1}{j}\frac{1}{p_{0m}\beta_{0m}J_1(p_{0m})} - \frac{1}{j}\frac{Z_0 w^2 d k}{8\pi^2 a^2} + \ldots\right] \times \frac{[J_0(P_{01}) + J_0(P_{02}) + \ldots]}{[J_1(P_{01}) + J_1(P_{02}) + \cdots + J_1(P_{11}) + J_1(P_{12}) + \ldots]} . \tag{48}$$

We have used the fact that $\sum \frac{1}{p_{0m}J_1(p_{0m})} = \frac{1}{2}$ to simplify the second term on the right-hand side of Eq. (48). In the case of a round hole with radius R, the second term, which we will call Z_2, reduces to

$$Z_2 = \frac{j Z_0 R^3 k}{\pi^2 a^2} \frac{[J_0(P_{01}) + J_0(P_{02}) + \ldots]}{[J_1(P_{01}) + J_1(P_{02}) + \cdots + J_1(P_{11}) + J_1(P_{12}) + \ldots]} . \tag{49}$$

This expression is similar to the one derived by Gluckstern[5] and Kurennoy,[6] but for the coefficient. We believe that the other terms are due to the contribution from the effects of the bounding wall of the pipe.

7.2 Impedance at High Frequencies

In the case of high frequencies, $k \gg \frac{p_{0m}}{a}$ and β_{0m} from Eq. (8) is real. Equation (46) can be written as

$$\begin{aligned} Z(\omega) &= \sum \frac{Z_0 w d k}{4\pi^2 a^2} \frac{[J_0(P_{01}) + J_0(P_{02}) + \ldots]}{[J_1(P_{01}) + J_1(P_{02}) + \ldots J_1(P_{11}) + J_1(P_{12}) + \ldots]} \frac{1}{p_{0m}\beta_{0m}J_1(p_{0m})} \\ &\quad \times [\cos(\beta_{0m} w) + j\sin(\beta_{0m} w)] \\ &= Z_r + j Z_i . \end{aligned} \tag{50}$$

The sign for β_{0m} should be chosen such that Z_r is positive for every m.

8.0 RESULTS AND DISCUSSION

Computations were performed for various slots and holes on a liner of inner radius $a = 0.0165$ m. The procedure consists of solving Eq. (15) for P_{0m}'s for given slot/hole dimensions. Equation (46) gives the impedance with the p_{0m}'s given by Eq. (6). The longitudinal coupling impedance of 3 slots of dimensions 4 mm × 4 mm, 4 mm × 2 mm, and 4 mm × 1 mm are shown in Figure 4(a) for low frequencies. The same results are shown in Figure 4(b) with the slot areas maintained the same; *i.e.*, the Z of the 4 mm × 2 mm slot was multiplied by 2, and that of the 4 mm × 1 mm slot was multiplied by 4. It is seen that the impedance per hole for the same pumping area decreases with the depth d of the slot.

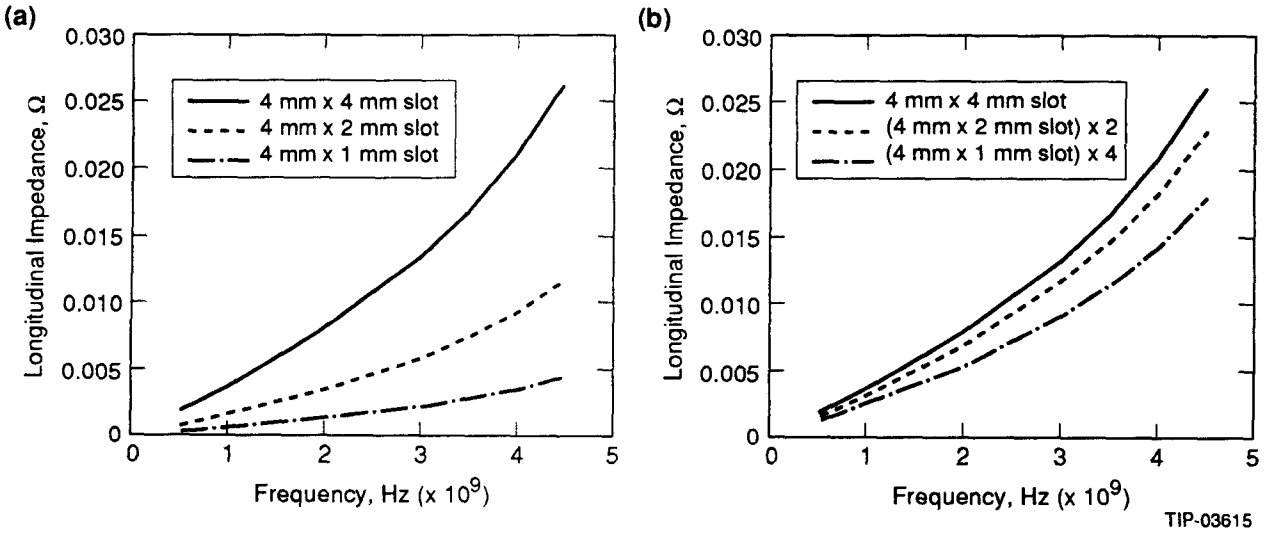

Figure 4. Impedance vs. Frequency for Slots of Various Sizes.

The coupling impedances for round holes of 4 mm, 3 mm, and 2 mm are shown in Figure 5 for the low frequency range. Also shown are the corresponding impedances Z_g, computed with the Gluckstern/Kurennoy formula. It is seen that the impedance from the present theory is mostly higher than the Gluckstern impedance; the difference is more pronounced for smaller hole sizes and higher frequencies. Chou and Barts[12] calculated impedances and wake potentials from MAFIA runs for the SSC liner. They show favorable comparisons of their wake potentials with that obtained using the Gluckstern formula for hole diameters ranging from 2 mm to 4 mm and at low frequencies. It should be recalled that we have used approximate boundary conditions at the slot. We have also halved the magnetic current at the slot assuming symmetry, used just the fundamental mode of propagation through the thickness of the slot, and ignored the boundary conditions at the far end of the slot at the bounding annular region. These differences should be anticipated.

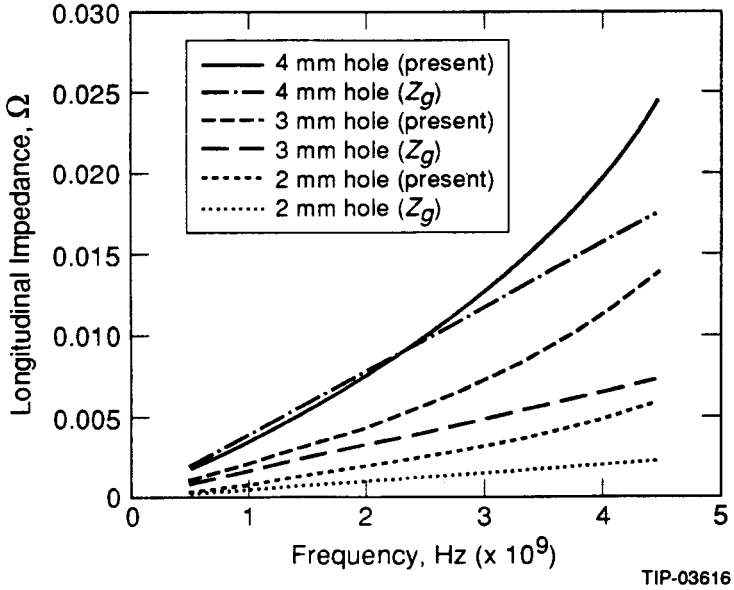

Figure 5. Impedance vs. Frequency for Holes of Various Sizes.

The impedances of square slots and round holes of similar dimensions are compared in Figure 6. The diffracted field from a square slot is found to be smaller than that from a round hole, but the round hole has a source area that is $\frac{\pi}{4}$ times less than that of the square hole. Due to these competing factors, the impedance of a slot is found to be slightly higher than that of a hole of the same dimension.

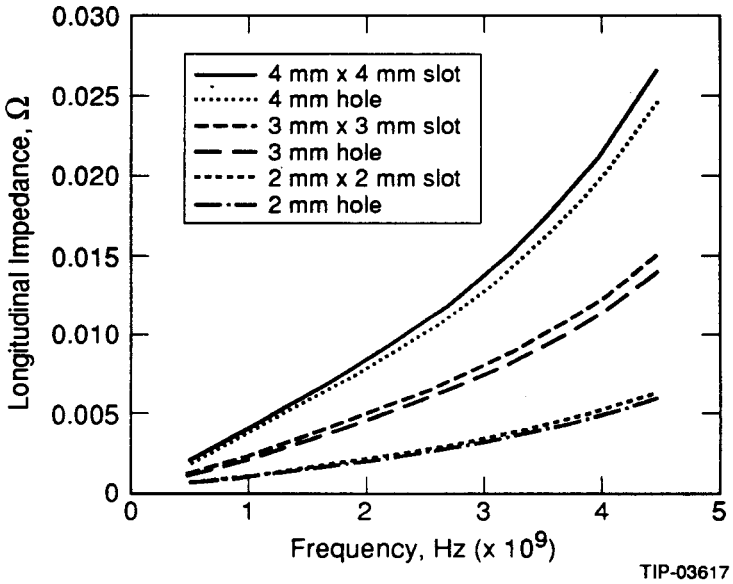

Figure 6. Impedance vs. Frequency—Slots and Holes Compared.

The real and imaginary part of impedances for 2-mm holes and for 4 mm × 2 mm slots for a frequency range of 0–60.0 GHz are shown in Figures 7 and 8. Resonant behavior

is observed at frequencies corresponding to each Bessel mode p_{0m}. At higher frequencies the behavior is sinusoidal, as shown in Eq. (50). The impedance is found to be infinity at every Bessel mode. This is due to the approximation we made in deriving Eqs. (19) and (20) from Eq. (18).

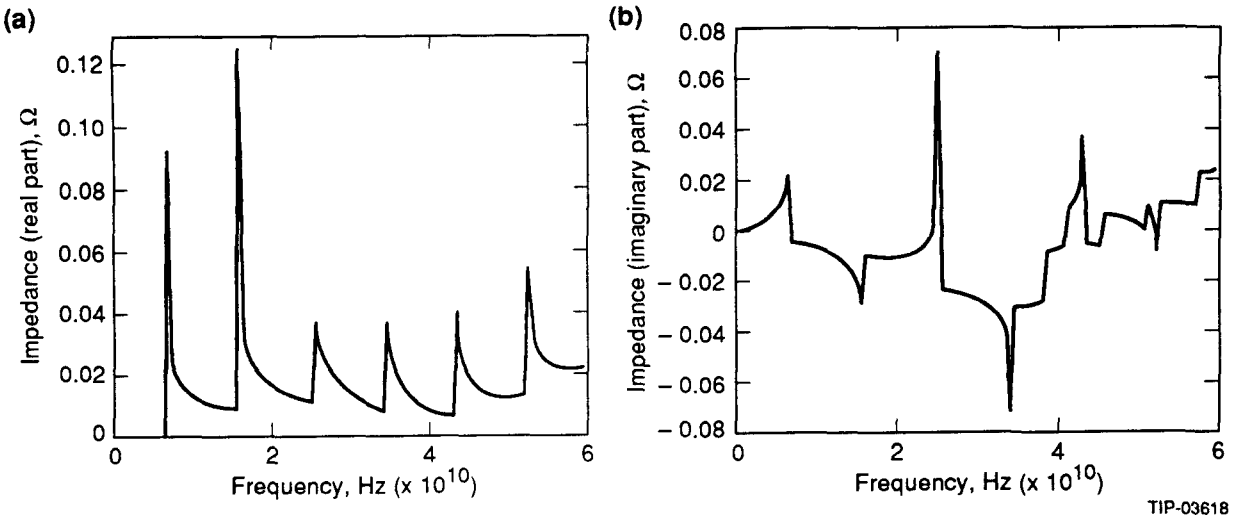

Figure 7. Longitudinal Impedance for 2-mm Hole. (a) Real part; (b) Imaginary part.

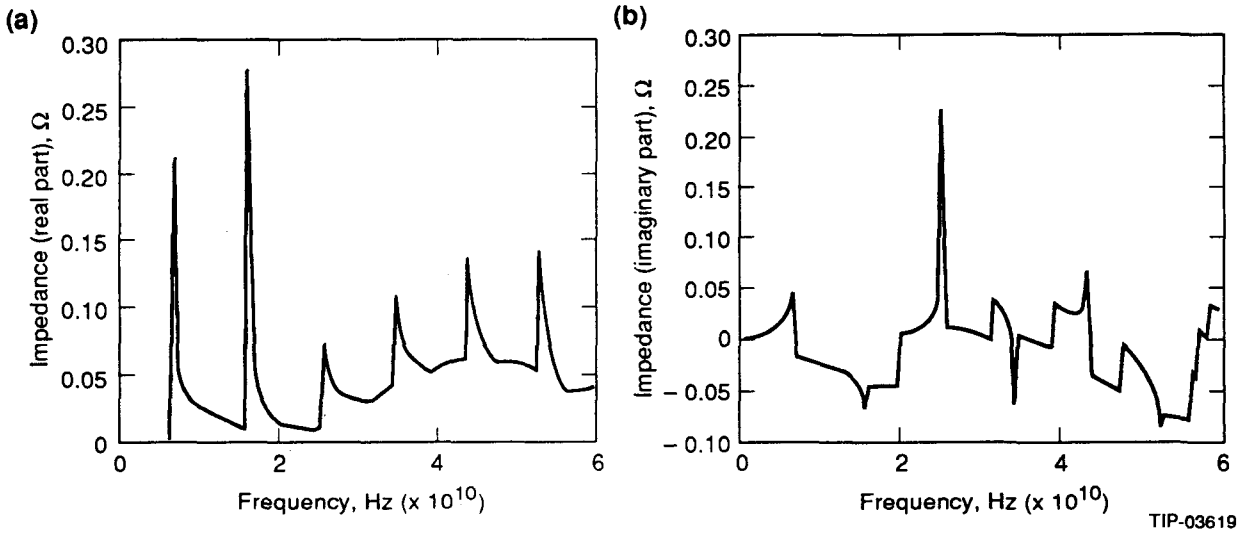

Figure 8. Longitudinal Impedance for 4 mm × 2 mm Slot. (a) Real part; (b) Imaginary part.

It should be noted that Eq. (48) for the impedance at low frequencies contains terms proportional to $\frac{wd}{a^2}$ and $\frac{w^2d}{a^2}$, *etc.* Kurennoy[6] shows that the low-frequency impedance for a slot is proportional to $\frac{wd^2}{a^2}$. His impedance was obtained using the polarizability for dielectric ellipsoids in the limit of very small aspect ratios, which in turn, was obtained from electrostatic considerations. The polarizabilities for slots of aspect ratios varying

from 0 to 1 and measured experimentally by Cohn[13] show a principal variation proportional to $w^2 d$. Hence, with this comparison, and since our analysis is kept electrodynamic throughout, we believe that the present method yields an impedance with the right dependence on slot dimensions for slots of various aspect ratios. In summary, we have obtained an expression for the longitudinal coupling impedance of slots/holes on the SSC Collider liner valid for a large range of frequencies with approximate boundary conditions at the slot/hole, and using waveguide normal mode analysis. Comparison with available analytical data is reasonable at low frequencies. Further work needs to be done toward improving the boundary conditions at the slot and building in the effect of the thickness of the slot, and in predicting the behavior of the impedance at frequencies corresponding to the Bessel modes.

ACKNOWLEDGEMENTS

The author acknowledges useful discussions with (and intensive criticism from) Weiren Chou, Alex Chao, and Sergey Kurennoy. The work was performed with encouragement from M.J. Syphers and W. Turner. The author is indebted to Jim Ellison and H.J. Weaver for discussions on some mathematical aspects.

REFERENCES

1. Bruno Zotter, "Electromagnetic Fields: Impedances and Wakes," *AIP Conference Proceedings 153*, Physics of Particle Accelerators, American Institute of Physics, 1987.
2. A.W. Chao, "Coherent Instabilities of a Relativistic Bunched Beam," Physics of High Energy Particle Accelerators, SLAC Summer School, 1982, AIP Conference Proceedings, No. 105, 1983.
3. S.S. Kurennoy, "Beam Chamber Coupling Impedance, Calculation Methods," CERN SL/91-31 (AP), 1991.
4. S.A. Heifets and S.A. Kheifets, "Coupling Impedance in Modern Accelerators," *Reviews of Modern Physics*, Vol. **63**, No. 3, July 1991.
5. R.L. Gluckstern, "Coupling Impedance of a Hole in a Thick Wall Beam Pipe," CERN SL/91 (AP), November 1991.
6. S.S. Kurennoy, "Beam Coupling Impedance of Holes in Vacuum-Chamber Walls," IHEP 92-84, UNK Div., Protvino, 1992.
7. J.D. Jackson, *Classical Electrodynamics*, John Wiley and Sons, New York, 1975.
8. T. Weiland, "MAFIA The Universal Software-System for Electromagnetic CAD," The MAFIA Collaboration, 1992.
9. R.E. Collin, *Field Theory of Guided Waves*, IEEE Press, 1991.
10. H.A. Bethe, "The Theory of Diffraction by Small Holes," *The Physical Review*, Second Series, Vol. **66**, Nos. 7 and 8, p. 163, 1944.
11. R. Plonsey and R.E. Collin, *Principles and Applications of Electromagnetic Fields*, McGraw-Hill Book Co., 1961.
12. W. Chou and T. Barts, "Wakefields and Impedances of a Perforated Liner," PMTN-0057C, Nov. 2, 1992, SSC Laboratory, Dallas, Texas.
13. S.B. Cohn, in *Microwave Filters, Impedance Matching Networks and Coupling Structures*, by G. Matthaei, L. Young, and E.M.T. Jones, p. 233, ARTECH House Books, 1980.